

MIT Open Access Articles

*pH sensing properties of graphene
solution-gated field-effect transistors*

The MIT Faculty has made this article openly available. **Please share** how this access benefits you. Your story matters.

Citation: Maily-Giacchetti, Benjamin, Allen Hsu, Han Wang, Vincenzo Vinciguerra, Francesco Pappalardo, Luigi Occhipinti, Elio Guidetti, Salvatore Coffa, Jing Kong, and Toma#s Palacios. "pH Sensing Properties of Graphene Solution-Gated Field-Effect Transistors." *Journal of Applied Physics* 114, no. 8 (2013): 084505. © 2013 AIP.

As Published: <http://dx.doi.org/10.1063/1.4819219>

Publisher: American Institute of Physics

Persistent URL: <http://hdl.handle.net/1721.1/87110>

Version: Final published version: final published article, as it appeared in a journal, conference proceedings, or other formally published context

Terms of Use: Article is made available in accordance with the publisher's policy and may be subject to US copyright law. Please refer to the publisher's site for terms of use.



pH sensing properties of graphene solution-gated field-effect transistors

Benjamin Maily-Giacchetti, Allen Hsu, Han Wang, Vincenzo Vinciguerra, Francesco Pappalardo, Luigi Occhipinti, Elio Guidetti, Salvatore Coffa, Jing Kong, and Tomás Palacios

Citation: *Journal of Applied Physics* **114**, 084505 (2013); doi: 10.1063/1.4819219

View online: <http://dx.doi.org/10.1063/1.4819219>

View Table of Contents: <http://scitation.aip.org/content/aip/journal/jap/114/8?ver=pdfcov>

Published by the [AIP Publishing](#)

Articles you may be interested in

[Indium arsenide nanowire field-effect transistors for pH and biological sensing](#)

Appl. Phys. Lett. **104**, 203504 (2014); 10.1063/1.4878659

[Hydrogen ion-selective electrolyte-gated organic field-effect transistor for pH sensing](#)

Appl. Phys. Lett. **104**, 193305 (2014); 10.1063/1.4878539

[Fabrication of high-performance graphene field-effect transistor with solution-processed Al₂O₃ sensing membrane](#)

Appl. Phys. Lett. **104**, 153506 (2014); 10.1063/1.4871865

[Improved sensing performance of polycrystalline-silicon based dual-gate ion-sensitive field-effect transistors using high-k stacking engineered sensing membrane](#)

Appl. Phys. Lett. **100**, 253703 (2012); 10.1063/1.4729762

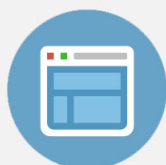
[Leaf-like carbon nanotube/nickel composite membrane extended-gate field-effect transistors as pH sensor](#)

Appl. Phys. Lett. **99**, 023108 (2011); 10.1063/1.3610554



Re-register for Table of Content Alerts

Create a profile.



Sign up today!



pH sensing properties of graphene solution-gated field-effect transistors

Benjamin Mailly-Giacchetti,¹ Allen Hsu,² Han Wang,² Vincenzo Vinciguerra,³ Francesco Pappalardo,³ Luigi Occhipinti,³ Elio Guidetti,⁴ Salvatore Coffa,³ Jing Kong,² and Tomás Palacios^{2,a)}

¹*Department of Materials Science and Engineering, Massachusetts Institute of Technology, Cambridge, Massachusetts 02139, USA*

²*Department of Electrical Engineering and Computer Science, Massachusetts Institute of Technology, Cambridge, Massachusetts 02139, USA*

³*STMicronics s.r.l, 95047 Catania, Italy*

⁴*STMicronics s.r.l, 20010 Castelletto, Italy*

(Received 21 July 2013; accepted 8 August 2013; published online 27 August 2013)

The use of graphene grown by chemical vapor deposition to fabricate solution-gated field-effect transistors (SGFET) on different substrates is reported. SGFETs were fabricated using graphene transferred on poly(ethylene 2,6-naphthalenedicarboxylate) substrate in order to study the influence of using a flexible substrate for pH sensing. Furthermore, in order to understand the influence of fabrication-related residues on top of the graphene surface, a fabrication method was developed for graphene-on-SiO₂ SGFETs that enables to keep a graphene surface completely clean of any residues at the end of the fabrication. We were then able to demonstrate that the electrical response of the SGFET devices to pH does not depend either on the specific substrate on which graphene is transferred or on the existence of a moderate amount of fabrication-related residues on top of the graphene surface. These considerations simplify and ease the design and fabrication of graphene pH sensors, paving the way for developing low cost, flexible, and transparent graphene sensors on plastic. We also show that the surface transfer doping mechanism does not have significant influence on the pH sensing response. This highlights that the adsorption of hydroxyl and hydronium ions on the graphene surface due to the charging of the electrical double layer capacitance is responsible for the pH sensing mechanism. © 2013 AIP Publishing LLC. [<http://dx.doi.org/10.1063/1.4819219>]

I. INTRODUCTION

Graphene, a two-dimensional material of sp²-bonded carbon atoms arranged in a honeycomb lattice, has attracted tremendous interest in the last few years due to its outstanding electrical, optical, and mechanical properties.^{1–3} Numerous electronic applications are being targeted by this material, including high frequency transistors,⁴ frequency multipliers⁵ and mixers,⁶ solar cells,⁷ and flexible displays.⁸ Furthermore, graphene, being an all-surface material with very high carrier mobility, is also very promising for chemical sensing applications^{9–11} that require high sensitivity, low noise, and a fast response. In addition, graphene grown by chemical vapor deposition (CVD) possesses the attractive advantage of enabling integration in large area and flexible substrates.¹² Specifically, solution-gated graphene field effect transistors have great potential to accurately detect pH^{9,10} as well as biomolecule sensing,^{13,14} and also to record cell activity.^{15,16}

Graphene-based chemical sensors also show an intricate response of their transfer characteristics to changes in electrolyte properties, such as salt concentration, type of ions, or pH.¹⁷ In addition, they could be expected to be sensitive to the substrate underneath and the amount of residues left on top of graphene during device processing; however, these two issues have not been studied in detail. And yet, in sensing experiments, the specific electric signal

from targeted biomolecules could be obscured by signal perturbations like substrate charging effects as well as charging effects of ionizable groups on residues at the graphene surface.^{17–19} Understanding the influence of these different elements on the sensor response will enable to improve the intrinsic graphene sensor response to targeted molecules.

In this article, after describing our fabrication methods for graphene solution-gated field-effect transistors (SGFETs) on SiO₂ and poly(ethylene 2,6-naphthalenedicarboxylate) (PEN) substrates, we compare the pH dependence and sensitivity of the electrical response of graphene SGFETs on these two substrates. We also compare the pH sensitivity of graphene-on-SiO₂ SGFETs that have either a moderate amount of fabrication-related residues on top of the graphene surface or a graphene surface completely clean of residues. These comparisons emphasize that the use of a flexible substrate as well as the presence of moderate amounts of organic residues on top of the graphene surface does not significantly influence the pH sensing mechanism. Finally, by fabricating graphene SGFETs on octadecyltrichlorosilane (OTS) substrate, we demonstrate that the surface transfer doping effect has a weak effect on the graphene pH sensing mechanism.

II. EXPERIMENTAL: FABRICATION METHODS

In this work, single-layer graphene films were grown by low-pressure CVD on copper foils.²⁰ Copper substrates are first annealed at 1000 °C at 350 mTorr in hydrogen gas to

^{a)}tpalacios@mit.edu.

remove native oxide and improve surface morphology. They are then exposed to CH_4 at 1.6 mTorr to initiate graphene growth. Raman characterization of the graphene film shows that it is more than 90% monolayer. Subsequently to the growth, a polymethyl methacrylate (PMMA) layer is coated on top of the graphene film and the copper substrate is etched away in copper etchant (CE-100 Transene). After cleaning in diluted HCl, the graphene film is transferred either on a Si/SiO₂ substrate or onto a PEN Teonex[®] (Teijin DuPont) substrate 125 μm thick. In order to study the influence of fabrication-related residues on pH sensing, two types of graphene SGFETs were fabricated: devices with a graphene surface completely clean of residues and devices with residues on top of the graphene surface. For the fabrication of graphene-on-SiO₂ transistors clean of residues, the removal of the PMMA layer was done by a high temperature anneal at 500 °C in H₂/Ar atmosphere that completely removes the PMMA layer and any residues left on the graphene surface. In the case of graphene-on-SiO₂ transistors with residues on top of the graphene surface as well as in the case of graphene-on-PEN transistors, in order to remove the PMMA layer, the transferred film was first exposed to acetone vapor to partly dissolve the PMMA layer while ensuring a good adhesion of the graphene to the substrate, and then the substrate was dipped in acetone to dissolve the remaining PMMA layer completely. This acetone cleaning process leaves a moderate amount of residues on top of graphene.

In the case of graphene-on-PEN transistors, prior to the graphene transfer, metal ohmic electrodes (Ni/Au, 20 nm/40 nm, Ni being used as the adhesion layer) were fabricated on the PEN substrate by a low temperature thin film metallization process, photolithography patterning, and subsequent

local wet etching of both Au and Ni layers. In the case of graphene-on-SiO₂ transistors, metal ohmic electrodes (Ti/Pt/Au, 2.5 nm/45 nm) were fabricated on the Si/SiO₂ substrate by photolithography patterning and e-beam evaporation of metals. This bottom-contact process ensures that the metal-graphene interface is clean of any polymer residue (e.g., PMMA) from the transfer process. Photoresist residue is typically found in top-contact electrodes, which increases the contact resistance.²¹ For the graphene patterning for graphene-on-SiO₂ transistors arrays, a thin layer of methyl methacrylate (MMA) was used as a protective layer spin-coated on the graphene. Subsequently, a layer of OCG 825 photoresist was spin coated. After defining the device structures with photolithography, the devices were isolated with an O₂ plasma etch. An acetone rinsing was then performed to remove the photoresist and the MMA layers. Finally, an annealing at 500 °C with H₂/Ar flow allowed the complete removal of the MMA residues left on the graphene surface as shown in Figure 1 below. For the purpose of the study of the influence of fabrication-related residues on pH sensing, the high temperature annealing was not performed in the case of graphene-on-SiO₂ transistors for which we purposely wanted to have the residues on top of the graphene surface.

Figure 1 shows the atomic force microscopy (AFM) images of graphene with and without residues on top at the end of the fabrication process of the graphene-on-SiO₂ transistors. It is worth noticing here that in the case where the graphene surface has residues on top, there is a high density of residue particles but the residues (i.e., mainly photoresist residues) do not form a continuous layer covering entirely the graphene surface. For the case of the graphene surface without residues, the root mean square (RMS) surface

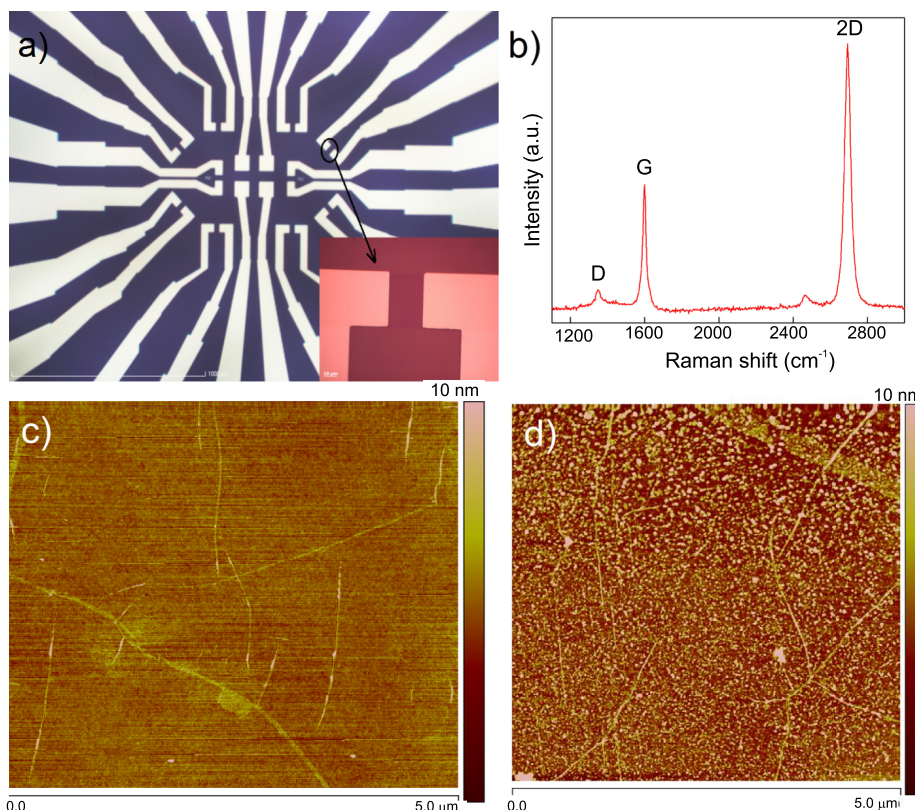


FIG. 1. (a) Optical micrograph of a sensor array on Si/SiO₂. The inset on the bottom right corner shows the detail of a CVD-grown graphene-on-SiO₂ transistor before depositing the insulation. (b) Raman spectrum for a wavelength $\lambda = 532$ nm confirms the presence of mono-layer graphene. (c) AFM image obtained with a Veeco Dimension 3100 system of the graphene surface for graphene-on-SiO₂ transistors that were fabricated with the method that completely cleans the graphene surface of any fabrication related residues. (d) AFM image of the graphene surface for graphene-on-SiO₂ transistors that were fabricated with the method that leaves organic residues on top of the graphene surface.

roughness is of the $5 \times 5 \mu\text{m}^2$ size image (0.65 nm), which is very close to the one of silicon dioxide without graphene on top ($\sim 0.4\text{--}0.5$ nm). In the case of the graphene surface with residues on top, there is an increase in RMS surface roughness (2.1 nm) compared to the case of very clean surface of graphene (0.65 nm).

After the fabrication of graphene transistors, the devices were integrated in a chip carrier and wirebonded for easy electrical characterization. We then covered the chip carrier and the transistor electrodes with silicone rubber (Dow Corning 370) in order to prevent the direct contact of the wires and most of the metal electrodes with the electrolyte. The leakage current between the gate electrolyte and the source contact was always negligible (~ 1 nA) thanks to this electrical insulation.

III. RESULTS AND DISCUSSION

A. Impact of fabrication-related residues on pH sensing

After fabrication, the devices were then immersed in a 10 mM phosphate buffer solution pH 7 with an ionic strength adjusted to 100 mM with sodium chloride. In all pH sensing experiments, aliquots of 0.5 M HCl and NaOH were added to change the pH of the solution. The solution was constantly stirred at 140 rpm. The SGFETs were gate biased by introducing an Ag/AgCl reference electrode into the solution in contact with the devices. To characterize the performance of the fabricated devices, the drain and source contacts of the graphene transistors, as well as an Ag/AgCl reference electrode, were connected to an Agilent 4155 Semiconductor Parameter Analyzer. The drain-source voltage V_{ds} was set to 50 mV, and the gate-source voltage V_{gs} sweep was limited in a window range of 0.5 V around the Dirac point to avoid the creation of surface defects as mentioned elsewhere.²²

First, the influence of resist residues left during photolithography processing on top of graphene was studied by comparing the pH sensitivity obtained for a graphene surface completely clean of residues and a graphene surface with residues on top.

The graphene-on-SiO₂ transistor transfer characteristics for a graphene with and without residues and their dependence with pH are shown in Figure 2.

In both devices, the Dirac point in the graphene transistor shifts linearly towards more positive voltages when the pH is increased. This allows pH sensing by measuring the graphene

electrical characteristics. The shift of the Dirac point is due to the increase in negative charge close to the graphene when the pH increases and indicates that the electrochemical double layer at the graphene/electrolyte interface is sensitive to pH allowing the capacitive charging of the surface by H₃O⁺ or HO⁻ ions.⁹ The more significant p-doping effect in graphene with a surface clean of residues is essentially attributed to the high temperature annealing used to clean the surface since we consistently observe in our devices a strong p-doping induced by high temperature annealing.

For a graphene surface with residues on top, the pH sensitivity is 21 mV/pH and in the case of a graphene surface clean of residues, the pH sensitivity is 22 mV/pH. Thus, these very similar pH sensitivities highlight that photoresist residues on top of graphene are not directly influencing the pH sensing mechanism. This observation opposes the hypothesis that the presence of ionizable acidic groups in resist residues could create pH-dependent surface charges in the vicinity of graphene responsible for the dependence of its electrical response with pH.¹⁷ This observation also simplifies the processing of graphene pH sensors since the presence of a reasonable amount of residues will not influence the pH sensitivity.

Besides, it is worth noticing that this sensitivity is quite similar to the one reported at the Dirac point for mechanically exfoliated graphene on SiO₂ (26 mV/pH)¹⁰ and for epitaxial graphene on silicon carbide (19 mV/pH).²² Similar sensitivity was also found in suspended graphene.¹¹

B. Impact of the use of a flexible substrate for pH sensing

In order to pave the way for flexible graphene pH sensors, the influence of a PEN substrate compared to a SiO₂ substrate was studied. Figure 3 illustrates the structure of a graphene-on-PEN transistor and shows its transfer characteristics, compared to a graphene-on-SiO₂ device.

The graphene transferred to both SiO₂ and PEN is p-doped as it is usually observed for graphene grown by CVD.^{23–25} However, graphene-on-SiO₂ is more p-doped than the one on PEN, which is attributed to the high temperature annealing performed during fabrication of graphene-on-SiO₂ transistors. The transconductance $g_m = \frac{\partial I_d}{\partial V_{gs}}$ is a key parameter determining the sensitivity of the sensor output (the drain-source current I_d) for a small variation of gate-source

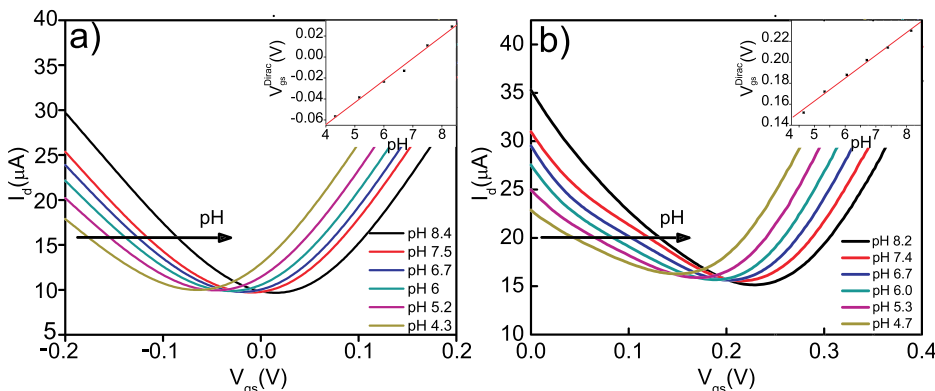


FIG. 2. Transfer characteristics of a $20 \times 40 \mu\text{m}^2$ graphene-on-SiO₂ SGFET at a constant drain-source voltage of $V_{ds} = 50$ mV for different pH (a) with a graphene surface completely clean of residues, (b) with residues on top of the graphene surface. Top-right corner insets show the linear relation between the shift at the Dirac point V_{gs}^{DIRAC} and the pH.

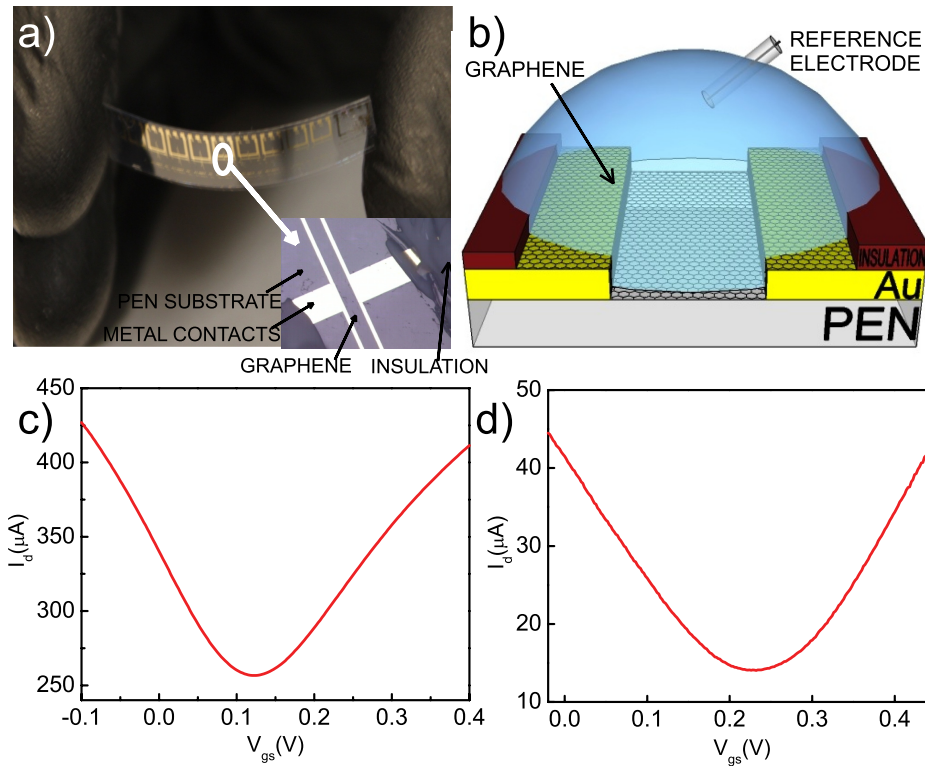


FIG. 3. (a) Optical image of an array of graphene chemical sensors on plastic substrate. The inset on the bottom right corner shows a detail of one of the devices. (b) Schematic illustration of a graphene-on-PEN solution-gated transistor. Transfer characteristics in a 10 mM phosphate buffer solution of (c) $20 \times 1000 \mu\text{m}^2$ graphene transistor on PEN as well as of (d) $20 \times 40 \mu\text{m}^2$ graphene transistor on SiO_2 for a drain-source voltage $V_{ds} = 50 \text{ mV}$.

voltage V_{gs} . The maximum transconductance of the graphene-on-PEN device is $1020 \mu\text{S}$ in the hole conduction regime and $716 \mu\text{S}$ in the electron conduction regime. When normalized by the transistor width, the maximum transconductance of the transistor is then 1 mS mm^{-1} , which is 5 times smaller than the transconductance of the reference graphene-on- SiO_2 devices. It should be noted that the transconductance for graphene on silicon dioxide is more than an order of magnitude higher than conventional planar silicon SGFET technology.^{23,26,27} This is due to the high interfacial capacitance²⁸ at the graphene/electrolyte interface as well as the high carrier mobility in graphene.²³

The higher transconductance in graphene-on- SiO_2 devices can be attributed to the higher carrier mobility on silicon dioxide than on PEN. Indeed, the field effect carrier mobility in a transistor μ_{FE} can be calculated using $\mu_{FE} = \frac{1}{C_{int}} \frac{\partial \sigma}{\partial V_{gs}}$, where C_{int} is the interfacial graphene/electrolyte capacitance and σ is the conductance. Following the interfacial capacitance model described in Ref. 28, we can extract a maximum carrier mobility of $300 \text{ cm}^2 \text{ V}^{-1} \text{ s}^{-1}$ for the graphene-on-PEN transistor and of $1250 \text{ cm}^2 \text{ V}^{-1} \text{ s}^{-1}$ for the graphene-on- SiO_2 transistor. The lower carrier mobility in the graphene-on-PEN devices is expected because the PEN substrate has more than 10 times higher RMS surface roughness ($\sim 5\text{--}10 \text{ nm}$) than SiO_2 ($\sim 0.4\text{--}0.5 \text{ nm}$), which increases carrier scattering and degrades graphene transport properties.²⁹

The dependence of the graphene-on-PEN transistor transfer characteristics with pH is shown in Figure 4.

As shown in Figure 4, the Dirac point shifts linearly with the pH, with a sensitivity of 22 mV/pH . The same sensitivity at the Dirac point was found with a transistor of size $100 \times 1000 \mu\text{m}^2$ confirming that the pH sensitivity is independent of the transistor size. The very similar sensitivity

values obtained in the graphene-on-PEN and graphene-on- SiO_2 devices highlight that the use of a flexible substrate does not significantly influence the electrical response of the devices to pH. Therefore, the pH response observed in our graphene transistors is not likely to arise from substrate charging effects of the silicon dioxide. This is contrary to what has been observed in Si/SiO_2 ion-sensitive field-effect transistors (ISFET), where the pH sensing mechanism comes from SiO_2 surface charging effects.³⁰ However, in the case of graphene, the absence of substrate charging effects is expected since graphene is believed to be impermeable to most gases and liquids,^{31,32} which would prevent the direct interaction of ions in the electrolyte with the substrate. In a

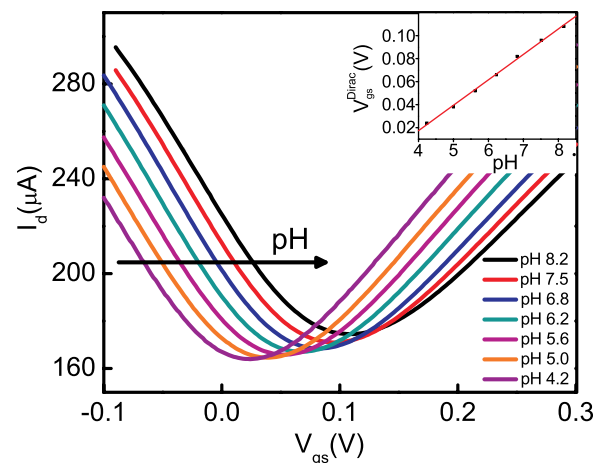


FIG. 4. Transfer characteristics of a $50 \times 1000 \mu\text{m}^2$ graphene-on-PEN SGFET at a constant drain-source voltage of $V_{ds} = 50 \text{ mV}$ for different pH values. Top-right corner inset shows the linear relation between the Dirac point shift V_{gs}^{Dirac} and the pH.

similar way, it has also been reported that the pH response of single-walled carbon nanotubes (SWNT) is not influenced by the substrate.¹⁹

In addition, the use of the graphene-on-PEN devices for real time monitoring of pH was also demonstrated. In these measurements, the voltage between gate and source was fixed first at $V_{gs} = 0.22$ V and in a second experiment set to $V_{gs} = -0.01$ V to show pH monitoring in both the hole and electron conduction regimes enabled by the ambipolar transport properties of graphene. As shown in Figure 5, the change in pH as a function of time is recorded as a change in the drain-source current I_d . The variations of I_d value with pH changes in both conduction regimes are consistent with the shift of the entire transfer characteristics curve. It should be noted that the pH sensing exhibits a good reversibility, although there is a small decrease in the current level after going down to very acidic pH.

C. Influence of the surface transfer doping effect on pH sensing

After showing that neither residues nor the substrate underneath graphene has significant influence in the pH sensing mechanism of our devices, the influence of a surface transfer doping effect was studied. Surface transfer doping is a mechanism that takes place in many gas-sensing experiments

with graphene.^{33–35} Indeed, some gas molecules when they adsorb on the graphene surface, it induces a charge transfer from the adsorbed gas molecules (or graphene) to graphene (or the adsorbed gas molecules). Therefore, a doping of the graphene sheet occurs through this surface charge transfer.^{33,36–38} In this mechanism, there is no electrostatic gating effect taking place as no gate bias can be applied to the gas.

To study the influence of surface transfer doping, graphene was transferred on an OTS substrate. According to Wang *et al.*,³⁹ the OTS substrate should reduce the chemical reactivity and the electron transfer reaction rate of graphene. Thus, if surface transfer doping has a significant influence in the pH sensing, a clear decrease in pH sensitivity should be observed for graphene-on-OTS SGFET.

OTS self-assembled monolayers were formed on a SiO_2 substrate, by exposing the substrate to an OTS solution (Sigma-Aldrich, 90%), diluted to 10 mM in toluene, overnight in a closed vial, then rinsed in fresh toluene and blown dry with nitrogen. Then, graphene was transferred on the substrate (which was already pre-patterned with the metal electrodes) and the fabrication technology described earlier for the graphene SGFET was performed in these devices.

The dependence of the graphene-on-OTS transistor transfer characteristics with pH is shown in Figure 6.

We observe that the graphene is slightly n-doped. This very small n-type doping can be attributed to the absence of high temperature annealing during fabrication and to the increased distance between the graphene and the charged impurities in SiO_2 due to the presence of the OTS layer that could further screen the charged impurities. A pH sensitivity of 18 mV/pH was found in this case, which is quite similar to the one obtained for graphene on SiO_2 . This result seems to support that surface transfer doping only has a weak effect in the pH sensing mechanism, at least under the conditions tested in this work.

Therefore, from all these pH sensing experiments, we can conclude that the electrostatic gating effect that induces

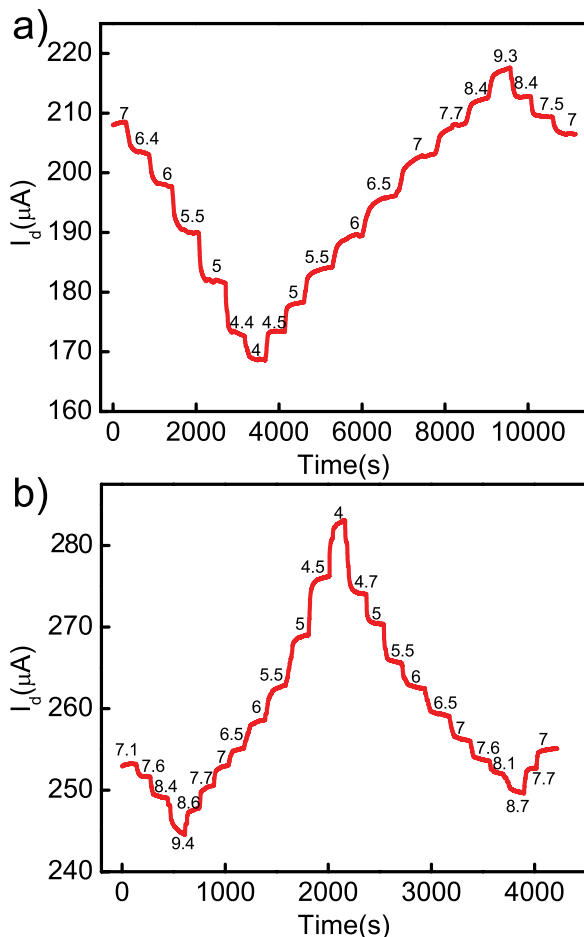


FIG. 5. pH monitoring with a $50 \times 1000 \mu\text{m}^2$ graphene-on-PEN SGFET by recording the drain-source current I_d versus time while changing the pH: (a) For a gate-source voltage $V_{gs} = 0.22$ V and (b) for $V_{gs} = -0.01$ V.

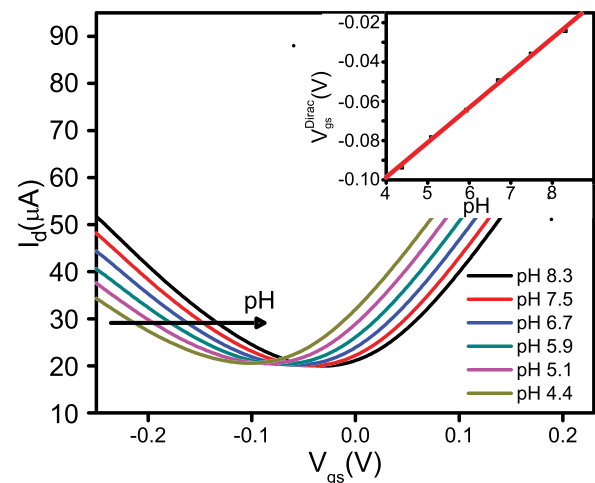


FIG. 6. Transfer characteristics of a $20 \times 40 \mu\text{m}^2$ graphene-on-OTS SGFET at a constant drain-source voltage of $V_{ds} = 50$ mV for different pH values. Top-right corner inset show the relationship between the Dirac point shift V_{gs}^{DIRAC} and the pH.

a specific adsorption of hydroxyl and hydronium ions at the graphene surface by capacitive charging of the electrical double layer is the main mechanism responsible for the pH sensitivity of graphene.⁹ This is in agreement with the theoretical study that shows that there is a specific adsorption of hydroxyl and hydronium ions at the graphene surface with gate bias in the solution.⁴⁰

IV. CONCLUSION

In summary, we demonstrated that graphene grown by CVD can be well integrated on plastic substrates for the fabrication of high performance pH sensors with the same pH sensitivity as on silicon dioxide. We further showed that neither the use of a flexible substrate nor the presence of moderate amounts of organic residues on top of graphene significantly influences the electrical response of graphene SGFETs to changes in pH. These considerations simplify and ease the fabrication of graphene pH sensors. Finally, we observed that surface transfer doping mechanism has only a weak influence on the pH dependence response of graphene SGFET, which highlights that the adsorption of hydroxyl and hydronium ions on the graphene surface due to the charging of the electrical double layer capacitance is responsible for the pH sensing mechanism.

ACKNOWLEDGMENTS

This work has been partially funded by the MIT-Army Institute for Soldier Nanotechnology, the Army Research Laboratory, and the International Iberian Nanotechnology Laboratory.

- ¹K. S. Novoselov, A. K. Geim, S. V. Morozov, D. Jiang, M. I. Katsnelson, I. V. Grigorieva, S. V. Dubonos, and A. A. Firsov, *Nature* **438**, 197–200 (2005).
- ²Y. Zhang, Y. W. Tan, H. L. Stormer, and P. Kim, *Nature* **438**, 201–204 (2005).
- ³K. S. Kim, Y. Zhao, Y. H. Jang, S. Y. Lee, J. M. Kim, K. S. Kim, J. H. Ahn, P. Kim, J. Y. Choi, and B. H. Hong, *Nature* **457**, 706–710 (2009).
- ⁴Y. M. Lin, K. A. Jenkins, A. Valdes-Garcia, J. P. Small, D. B. Farmer, and P. Avouris, *Nano Lett.* **9**, 422–426 (2009).
- ⁵H. Wang, D. Nezich, J. Kong, and T. Palacios, *IEEE Electron Device Lett.* **30**, 547–549 (2009).
- ⁶H. Wang, A. Hsu, J. Wu, J. Kong, and T. Palacios, *IEEE Electron Device Lett.* **31**, 906–908 (2010).
- ⁷X. Wang, L. Zhi, and K. Mullen, *Nano Lett.* **8**, 323–327 (2008).
- ⁸V. P. Verma, S. Das, I. Lahiri, and W. Choi, *Appl. Phys. Lett.* **96**, 203108 (2010).
- ⁹P. K. Ang, W. Chen, A. T. Wee, and K. P. Loh, *J. Am. Chem. Soc.* **130**, 14392 (2008).
- ¹⁰Y. Ohno, K. Maehashi, Y. Yamashiro, and K. Matsumoto, *Nano Lett.* **9**, 3318–3322 (2009).

- ¹¹Z. Cheng, Q. Li, Z. Li, Q. Zhou, and Y. Fang, *Nano Lett.* **10**, 1864–1868 (2010).
- ¹²S. Bae, H. Kim, Y. Lee, X. Xu, J. S. Park, Y. Zheng, J. Balakrishnan, T. Lei, H. R. Kim, Y. I. Song, Y. J. Kim, B. Ozyilmaz, J. H. Ahn, B. H. Hong, and S. Iijima, *Nat. Nanotechnol.* **5**, 574–578 (2010).
- ¹³Y. Ohno, K. Maehashi, and K. J. Matsumoto, *J. Am. Chem. Soc.* **132**, 18012 (2010).
- ¹⁴X. Dong, Y. Shi, W. Huang, P. Chen, and L. J. Li, *Adv. Mater.* **22**, 1649–1653 (2010).
- ¹⁵V. Cohen-Karni, Q. Qing, Q. Li, Y. Fang, and C. M. Lieber, *Nano Lett.* **10**, 1098–1102 (2010).
- ¹⁶L. H. Hess, M. Jansen, V. Maybeck, M. V. Hauf, M. Seifert, M. Stutzmann, I. D. Sharp, A. Offenhausser, and J. A. Garrido, *Adv. Mater.* **23**, 5045–5049 (2011).
- ¹⁷I. Heller, S. Chatoor, J. Mannik, M. A. Zevenbergen, C. Dekker, and S. G. Lemay, *J. Am. Chem. Soc.* **132**, 17149–17156 (2010).
- ¹⁸Y. Dan, Y. Lu, N. J. Kybert, Z. Luo, and A. T. Johnson, *Nano Lett.* **9**, 1472–1475 (2009).
- ¹⁹J. H. Back and M. Shim, *J. Phys. Chem. B* **110**, 23736–23741 (2006).
- ²⁰X. Li, W. Cai, J. An, S. Kim, J. Nah, D. Yang, R. Piner, A. Velamakanni, I. Jung, E. Tutuc, S. K. Banerjee, L. Colombo, and R. S. Ruoff, *Science* **324**, 1312–1314 (2009).
- ²¹A. Hsu, H. Wang, K. K. Kim, J. Kong, and T. Palacios, *IEEE Electron Device Lett.* **32**, 1008–1010 (2011).
- ²²J. Ristein, W. Zhang, F. Speck, M. Ostler, L. Ley, and T. Seyller, *J. Phys. D* **43**, 345303 (2010).
- ²³L. H. Hess, M. V. Hauf, M. Seifert, F. Speck, T. Seyller, M. Stutzmann, I. D. Sharp, and J. A. Garrido, *Appl. Phys. Lett.* **99**, 033503 (2011).
- ²⁴J. Bai, L. Liao, H. Zhou, R. Cheng, L. Liu, Y. Huang, and X. Duan, *Nano Lett.* **11**, 2555–2559 (2011).
- ²⁵T. O. Wehling, A. I. Lichtenstein, and M. I. Katsnelson, *Appl. Phys. Lett.* **93**, 202110 (2008).
- ²⁶S. Ingebrandt, C. Yeung, W. Staab, T. Zetterer, and A. Offenhausser, *Biosens. Bioelectron.* **18**, 429–435 (2003).
- ²⁷A. Offenhausser, C. Sprossler, M. Matsuzawa, and W. Knoll, *Biosens. Bioelectron.* **12**, 819–826 (1997).
- ²⁸M. Dankerl, M. V. Hauf, A. Lippert, L. H. Hess, S. Birner, I. D. Sharp, A. Mahmood, P. Mallet, J.-Y. Veuillen, M. Stutzmann, and J. A. Garrido, *Adv. Funct. Mater.* **20**, 3117 (2010).
- ²⁹C. Dean, A. Young, I. Meric, C. Lee, L. Wang, S. Sorgenfrei, K. Watanabe, T. Taniguchi, P. Kim, and K. Shepard, *Nat. Nanotechnol.* **5**, 722–726 (2010).
- ³⁰P. Bergveld, in *IEEE Sensor Conference*, Toronto (2003), Vol. 10, p. 1.
- ³¹J. S. Bunch, S. S. Verbridge, J. Alden, A. M. Van Der Zande, J. M. Parpia, H. G. Craighead, and P. L. McEuen, *Nano Lett.* **8**, 2458–2462 (2008).
- ³²O. Leenaerts, B. Partoens, and F. Peeters, *Appl. Phys. Lett.* **93**, 193107 (2008).
- ³³H. Liu, Y. Liu, and D. Zhu, *J. Mater. Chem.* **21**, 3335–3345 (2011).
- ³⁴I. Gierz, C. Riedl, U. Starke, C. R. Ast, and K. Kern, *Nano Lett.* **8**, 4603–4607 (2008).
- ³⁵F. Schedin, A. K. Geim, S. Morozov, E. W. Hill, P. Blake, M. I. Katsnelson, and K. S. Novoselov, *Nature Mater.* **6**, 652–655 (2007).
- ³⁶T. Wehling, K. Novoselov, S. Morozov, E. Vdovin, M. Katsnelson, A. Geim, and A. Lichtenstein, *Nano Lett.* **8**, 173–177 (2008).
- ³⁷O. Leenaerts, B. Partoens, and F. Peeters, *Phys. Rev. B* **77**, 125416 (2008).
- ³⁸A. Lherbier, X. Blase, Y. Niquet, F. Triozon, and S. Roche, *Phys. Rev. Lett.* **101**, 36808 (2008).
- ³⁹Q. H. Wang, Z. Jin, K. K. Kim, A. J. Hilmer, G. L. C. Paulus, C. Shih, M. H. Ham, J. D. Sanchez-Yamagishi, K. Watanabe, and T. Taniguchi, *Nat. Chem.* **4**, 724–732 (2012).
- ⁴⁰D. J. Cole, P. K. Ang, and K. P. Loh, *J. Phys. Chem. Lett.* **2**, 1799–1803 (2011).